Attrition of Lime Sorbents During Fluidization in a Circulating Fluidized Bed Absorber

ARTICLE *in* INDUSTRIAL & ENGINEERING CHEMISTRY RESEARCH · NOVEMBER 1993

Impact Factor: 2.59 · DOI: 10.1021/ie00023a044

4 AUTHORS, INCLUDING:

Tim C. Keener
University of Cincinnati
196 PUBLICATIONS **1,172** CITATIONS

SEE PROFILE

Attrition of Lime Sorbents during Fluidization in a Circulating Fluidized Bed Absorber

Sang-Kwun Lee,[†] Xiaolin Jiang,[*,†,‡] Tim C. Keener,[*,†] and Soon J. Khang[§]

Department of Civil and Environmental Engineering and Department of Chemical Engineering, The University of Cincinnati, Cincinnati, Ohio 45221

The experimental data of lime sorbent attrition obtained from mechanical and thermal attrition tests in a circulating fluidized bed absorber (CFBA) are represented. The results indicate that the predominant attrition mechanism during lime fluidization is surface abrasion due to collisions of the parent solids in a bed. Attrition of lime at higher temperatures decreased due to its hardened properties with rising temperature, while such solids as limestone become more attritable by the crepitation resulting from the increased internal pressure. With an introduction of the minimum weight of parent solids, the attrition rate of lime in a CFBA has a first-order dependency with respect to time. The attrition rate constant is expressed in an Arrhenius form, using the kinetic model which relates the attrition rate to the gas properties such as temperature and molecular weight and the geometry of the fluidized bed as well as the fluidization velocity. The experimental data obtained from these tests in a CFBA agree well with the attrition model, and the model indicates trends due to increased temperature considering thermal attrition. From the model the attrition activation energy, E_a and k_o, can be obtained as $E_a = 3.383 \times 10^{-3}$ kJ/kg and $k_o = 1.29 \times 10^{-4}$ s^{-1}. Comparisons of the mechanical and thermal attrition data obtained experimentally with the theoretical values computed with the attrition activation energy, E_a and k_o, are in good agreement, and thus the results may be applicable to lime attrition in a fluidized bed.

Introduction

A number of investigators (Borgwardt and Bruce, 1986; Kirchgessner et al., 1987) have concluded that one of the primary mechanisms in poor sorbent utilization of dry sorbent injection processes for flue gas desulfurization (FGD) is the fact that the products of the SO_2–sorbent reaction have such large molar volumes that they plug the pores necessary for SO_2 diffusion into the unreacted core. The thin product layer of impervious material prevents the fresh portion of the solid sorbent from being exposed to SO_2. Therefore, removal of the layer of product from the sorbent exterior would result in greater utilization of the sorbent. A circulating fluidized bed absorber (CFBA) employs a relatively high fluidization velocity and thus has a strong fluid-induced mechanical force sufficient to attrit the solid sorbents during fluidization. In other words, a significant size reduction of sorbents occurs due to attrition during fluidization. As a result, the removal of the product layer covering the unreacted sorbent by attrition allows the surrounding SO_2 to contact with the fresh sorbent surface continuously and leads to an increase of sorbent utilization. Therefore, identifying attrition mechanisms in reactors such as the CFBA would allow for better process optimization and increased sorbent utilization, which would result in less volume of waste material generated.

In a CFBA, a bed of sorbent solids is reacted with SO_2 in the flue gas to produce solid products. Previous results with a CaO sorbent (Jiang, 1991; Keener et al., 1991) have shown that water addition in the form of water directly sprayed onto the bed significantly enhances SO_2 uptake and can lead to sorbent utilization values of over 90%. This is considered to be caused by the *in situ* hydration of the lime particles and the resultant high reactivity of the moist hydrated lime. Reaction products which form on the surface of the partially hydrated lime particles are also subject to attrition in the intense agitation which describes the particle environment in these reactors.

While the effects of attrition are significant in many other FGD processes, the underlying attrition mechanisms have been rarely studied in a systematic fashion. Lime is the primary sorbent used in the proposed CFBA system, and its attrition can influence the particle size distribution which is subsequently available for reaction with SO_2 by means of hydration. In the proposed CFBA, however, a number of other products will be formed including $Ca(OH)_2$, $CaSO_3$, and $CaSO_4$, whose attrition rates will differ from that of CaO. This paper represents the experimental findings obtained from a study of attrition of a lime sorbent with the objective to find which mechanisms are predominant in the attrition of solids during fluidization in a CFBA and if an expression which describes this type of attrition can be developed. It is anticipated that these findings may be expanded to include a description of attrition of the other products in the future and thus aid in the optimization of the system.

Previous Work

The factors which affect attrition dynamics include the properties of the sorbents (particles), the influence of the reactor environment, and the types of breakage mechanics which dominate for the particle–reactor system (Bemrose and Bridgwater, 1987). The properties of particles such as size, surface, porosity, hardness, cracks, density, shape, and particle strength strongly affect the attrition rate. The force required to induce plastic behavior in solids is known as the yield stress and is sometimes defined as the material's strength (British Materials Handling Board, 1987), although the stress at which the particle ruptures is a more useful measure of particle strength with respect to particle attrition. This definition of particle strength has been explained in terms of particle properties such as density, Poisson's ratio, and Young's modulus (which are assumed to be independent of particle size) and the relative

* To whom correspondence should be addressed.
† Department of Civil and Environmental Engineering.
‡ Present address: Noell, Inc., Herndon, VA 22071.
§ Department of Chemical Engineering.

0888-5885/93/2632-2758$04.00/0

velocity between the particle and a target (British Materials Handling Board, 1987). Attrition rate is also dependent upon time, velocity, pressure, shear, temperature, viscosity, and turbulence in a system. In addition, the extent of attrition varies depending on which breakage mechanism is dominant. Typically, attrition due to abrasion causes less attrition than such mechanisms as shattering, fracture, and grinding.

The shape of the particle influences the behavior of the particle when subjected to external forces through the distribution of the stresses within the solid. Spherical particles are less likely to attrit than irregularly shaped particles. The size of the particle and the size distribution of the entire particle population also influence attrition. In general, larger particles are more easily attritted than smaller ones. This is attributed to the presence of fewer faults, flaws, or discontinuities in smaller particles. However, there is no systematic relationship between particle size, size distribution, and friability (British Materials Handling Board, 1987). The porosity of the particle influences its friability. In general, porous particles are more resilient than nonporous particles of similar size and thus attrit less. Decrepitation (breakdown in particle size due to internal forces, generally induced by heating) may be responsible for particle attrition of porous solids subjected to sudden extreme changes in temperature. Also, pores filled with liquids are more likely to rupture due to changes in state of the liquid caused by temperature or pressure changes. The surface roughness of the particle also affects the rate of production of *fines*. These fines, the characteristic product of abrasion processes, are formed from the wearing away of the surface *peaks* of the particles. The particle hardness provides a general measure of the particle's ability to resist wear and to its susceptibility to fracture.

The influence of the reactor environment (Bemrose and Bridgwater, 1987) along with the properties of the solids, as discussed above, determine the extent of attrition. The variables which have been shown to influence attrition within the reactor include the time of exposure, the particle velocity, the temperature and pressure of the system, and the type of enclosure (i.e., hard surface or soft). In solid transport systems such as screw conveyers, shear caused by movement of one layer of particles over another layer of particles or solid surface is the major cause of degradation. In reactors such as a boiler duct work where sorbent is to be injected, the large temperature gradients experienced by the sorbents upon injection could influence attrition.

The mechanics which govern attrition are complex (British Materials Handling Board, 1987). The systems of stresses and strains which act on a particle are difficult to measure quantitatively or assess qualitatively. In terms of uniaxial compression and pure shear, some methods are available for determining relative measures of strength or resistance. A number of quantitative expressions have been developed to measure such properties as the particle strength (Hooke's Law), the particle tendency to fracture through crack propagation, and the energy required to break particles (e.g., Rittinger's law). Two areas which have not been studied as extensively are decrepitation by thermal shock and breakage by gas–solid reactions (Keener et al., 1991).

In a fluidized bed, attrition of particles has been considered as the result of disruptive stresses acting on the particles (Ulerich et al., 1980; Vaux and Fellers, 1981; Shamlou et al., 1990). The main sources of these stresses causing particle attrition are fluid dynamic induced stresses such as high and low velocity impacts, chemical stresses due to chemical reactions, and thermal stresses resulting in changes of internal pressure. However, the attrition behavior of the bed material is made difficult by the interaction and competition between these various causes of attrition; no comprehensive model so far is available for assessing the attrition phenomena quantitatively. Attrition studies (Keener et al., 1991; Bemrose and Bridgwater, 1987) have mostly been limited to special processes. These studies have generally been undertaken with carbons or limestones that do not fracture or abrade readily. In addition, most attrition models relate the size or weight reduction of particles to the energy input to the specific system.

Merrick and Highley (1974) found that the size distribution of fines produced was approximately constant for a particular bed material and independent of bed size distribution or operating conditions. They developed an attrition model based on Rittinger's law, in which the attrition of ash in a fluidized bed combustor (FBC) is proportional to the excess gas velocity ($U - U_{mf}$) and the weight of bed material, W. The generation of carbon fines by attrition during the fluidized combustion of a bituminous coal has been studied with a 140-mm-i.d. fluidized bed combustor with variable excess air, bed temperature, fluidizing gas velocity, and size of sand and coal by Arena et al. (1983). Their results indicated that attrition of carbon in a fluidized bed combustor (FBC) is directly proportional to the product of the excess gas velocity above the minimum fluidization velocity and the overall carbon surface exposed to attrition inside the bed. The attrition rate constant is affected by the size of sand used and (particularly with finer coal) by bed temperature. Chirone et al. (1984) similarly investigated the generation of fines due to the abrasion of bed solids on the surface of burning particles in 40-mm-i.d. fluidized bed combustors. They found that combustion enhances attrition, resulting in an increase of fine generation when fluidizing batches of petroleum coke, and that the shape of the attrition curves has a peak value of attrition rate between the beginning of combustion and burnout. They related the peak of attrition rate to the opposite effects of surface activation, which leads to an increased concentration of asperities, and particle shrinkage resulting in the reduction of the surface. The attrition rate of char particles in a char/sand fluidized bed was obtained experimentally by Lin et al. (1980). They correlated the attrition rate to an exponential function as $k_a = 2.81 \times 10^{-3} \exp[0.162(U - U_{mf})]$.

Ulerich et al. (1980) studied the attrition of limestone in the bubbling upper zone of a fluidized bed combustor. They found that the rate of attrition decreases monotonically to a steady-state rate, and that the attrition rate is proportional to the excess bubble velocity. Shamlou et al. (1990) investigated the hydrodynamic influences on particle breakage in fluidized beds and described the rate of generation of fines. They observed the continuous decrease of the agglomerates with 5% binder concentration during fluidization at the velocity of $1.2U_{mf}$. The attrition rate constant, k_a, was interpreted as a first-order dependency with respect to the excess gas velocity above the minimum fluidization velocity under low-energy impacts in the bulk of the fluidized bed. But their experimental data failed to describe the high impact model developed for the distributor region.

The kinetic, thermal, and chemical attrition rate constants of $MnCl_2$ in a fluidized bed were experimentally correlated as functions of gas velocity and minimum

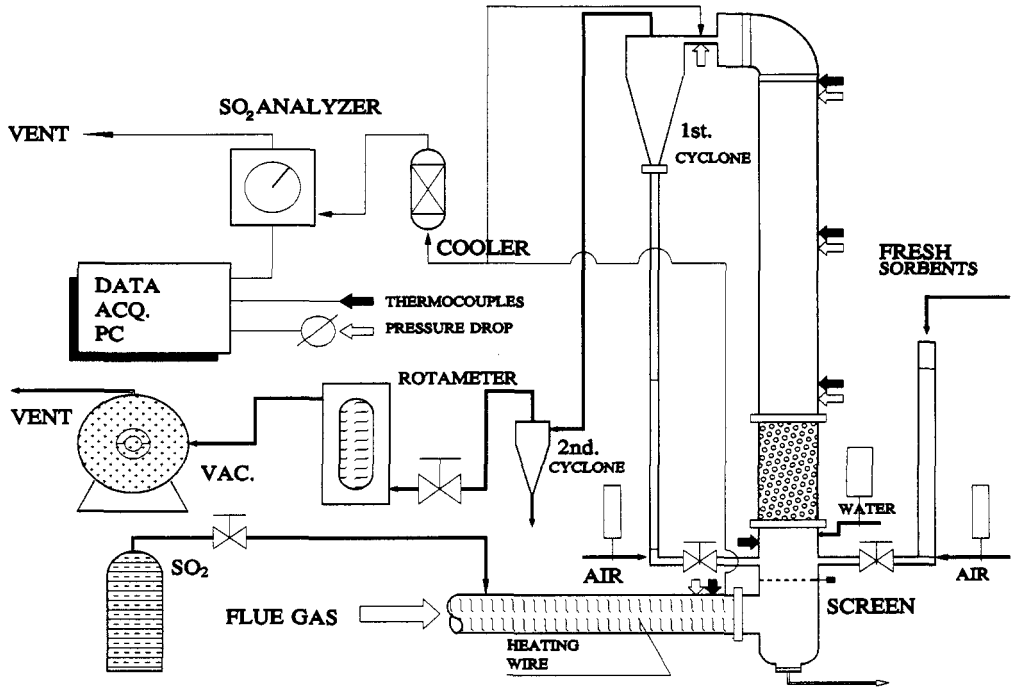

Figure 1. Scheme of bench scale CFBA unit.

fluidization velocity or temperature by Flamant and Chraibi (1989). The results showed a smooth increase of attrition with rising temperature within 300 °C and a rapid increase at temperatures greater than 300 °C. The degree of thermal attrition obtained from these experiments was 1 order of magnitude larger than kinetic attrition or chemical attrition. They also reported that a similar trend was observed for other materials of which the rate constants may differ. Jiang (1991) also examined the chemical attrition of lime in a CFBA with water injection. His results suggested that over a certain critical moisture content in the bed material, the weight loss occurs extremely rapidly, resulting from shattering of the hydrated lime. He concluded that the shattering mechanism resulting from wetting of the lime particles may cause much more attrition than the abrasion mechanism dominant under dry conditions and that the attrition rate is strongly dependent upon the approach to saturation temperature under wet conditions. The correlation between the attrition rate constant, k_w, under wet conditions and approach to saturation temperature, Δt was obtained as $k_w = 0.021 - 0.00017\Delta t$.

Experimental Section

Experimental System. The attrition tests were conducted in a bench-scale CFBA unit which was primarily constructed for the purpose of studying sulfur uptake of solid sorbents under low-temperature conditions. The bench-scale CFBA unit, which is similar in design to a pilot scale unit built earlier (Keener et al., 1988), consists of a bed reactor of 76.2 mm in diameter and 3 m in length, two high-efficiency cyclones for gas/solid separation, sorbent injection and recycling system, water injection system, gas heating system, and gas flow, concentration, temperature, and pressure monitoring system. The CFBA unit is schematically shown in Figure 1.

The bed reactor was built with 1.83 m of steel pipe and 1.22 m of Pyrex glass, which allows for visible observation of the solid mixing during the fluidization. A woven stainless steel mesh (mesh no. 70) at the base of the bed serves to distribute the gas flow and support the sorbent materials.

The sorbent injection and recycling systems were also designed to be checked visibly for maintaining constant feeding and recycling rate for the case of continuous operation. The sorbent injection system consists of a pneumatically operated L-valve which is controlled by air flow. The coarse sorbent entrained from the bed is captured by the two cyclones. Two high-efficiency cyclones with diameters of 0.061 m (first cyclone) and 0.038 m (second cyclone) collect solids greater than 32 μm with 99.9% efficiency, and particles greater than 10 μm with 97.9% efficiency, respectively. The collected sorbents are recirculated to the base of the reactor through another L-valve.

The gas heating and conditioning system provides the simulated flue gas ranging from 150to 250°C by means of a heater located at the bottom of the reactor. The simulated flue gas used in this study did not contain gas-phase concentrations of CO_2 and H_2O at the levels found in typical flue gases. As will be discussed later, the degree of attrition of CaO is to be expected to be influenced by these constituents. While the absolute degree of attrition of CaO as reported in this study may not coincide with those obtained from experiments using actual flue gases, it is believed that the overall trends will be the same. For sulfation tests, sulfur dioxide of 3000 ppm is injected to simulate the flue gas emitted from the combustion of high sulfur coal available in Ohio.

Sampling ports are positioned at both the top and the bottom of the reactor, and pressure taps and thermocouples are installed at equal distances throughout the height of the fluidized bed. The particulate samples can be taken from both the bed and the two cyclones in order to measure the weight and size changes during fluidization. All the gas concentrations, temperatures, and pressures measured at selected locations along the bed are monitored and recorded continuously by a data acquisition system.

Materials and Experimental Procedure. Two discrete ranges of commercially available lime were used as solid sorbents for attrition tests. One ranged between 1095 μm (16 mesh) and 2380 μm (8 mesh) in diameter and the other ranged between 595 μm (30 mesh) and 1095 μm (16 mesh). The lime samples were about 1.3 cm in diameter.

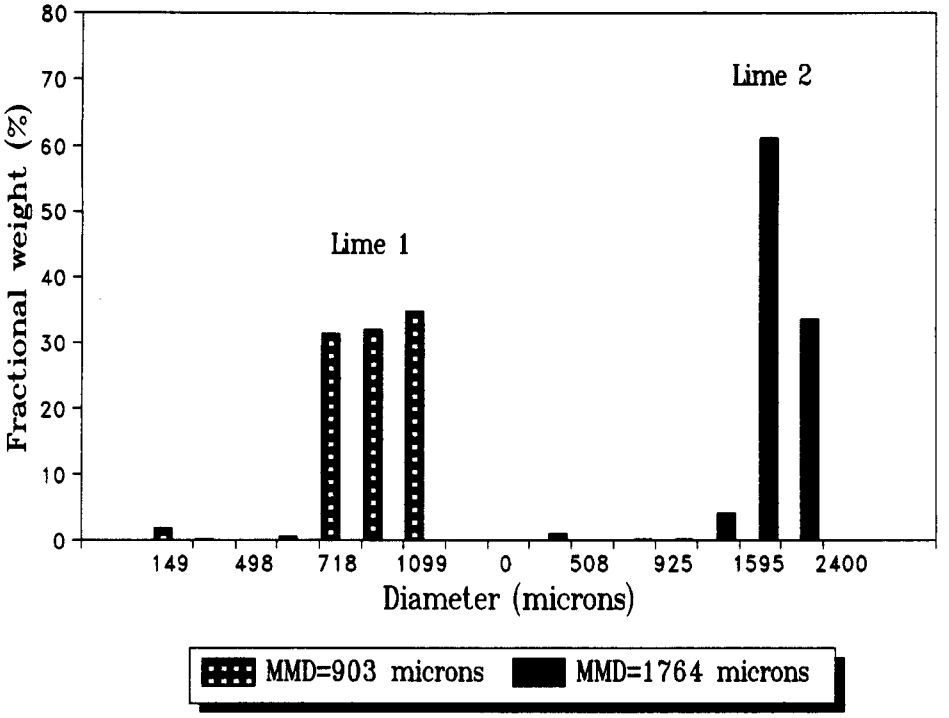

Figure 2. Fractional size distribution of lime samples.

Table I. Physical Properties[a] of Lime Samples

sample no.	mass mean diameter (μm)	mean diameter (μm)	BET surface area (M^2/kg)	pore vol (m^3/kg)	bulk density (kg/m^3)
lime 1	1764	1682	1.27×10^3	0.33×10^3	1.45×10^3
lime 2	903	820	1.36×10^3	0.42×10^3	1.28×10^3

[a] Measured.

Table II. Chemical Properties of Lime Samples[a]

chemical components	wt (%)	chemical components	wt (%)
total CaO	93	CO_2	1.1–1.2
avail CaO	87.5–88.5 (95[b])	H_2O	0.4
MgO	2.65–2.75	S_1O_2	1.95–2.05
sulfur	0.045–0.050		

[a] Obtained from Dravo Lime Co. [b] Measured.

The sorbents, therefore, were ground by means of a pulverizer (Bico Co.) to two mass mean diameters (MMD) of 903 and 1764 μm. The size distributions for the lime samples are shown in Figure 2.

The parent lime sample is a high calcium quicklime formed by calcining limestone so that CO_2 is liberated. The available lime measured was 95%, and a slaking test indicated the lime to be very reactive. The physical and chemical properties of the lime samples are measured, or obtained from the supplier (Dravo Co.), and the results are summarized in Tables Iand II , respectively. [The surface area of the lime studied here is below that of typical limes used for wet FGD application. However, lime of this type has been used in previous CFBA tests with good results (Jiang, 1991) in terms of sorbent utilization.]

Attrition tests were carried out in the circulating fluidized bed absorber (CFBA) with the narrowly sieved lime samples of 1764 μm (lime 1) and 903 μm (lime 2) mass mean diameters (MMD). The fluidizing gas was air with superficial velocities of 2 m/s for the lime of 903 μm and 3–5 m/s for the lime of 1764 μm, respectively. Since the gas velocities were much less than the terminal velocities (11 m/s for lime 1 and 7 m/s for lime 2) of the lime samples, no elutriation of the parent solids was expected during fluidization. The weight reduction of bed materials during fluidization may, therefore, be considered as a result of attrition. The gas temperature ranged between 20 °C for the mechanical attrition tests and 65–177 °C for the thermal attrition tests. The gas velocity and temperature for the attrition tests were maintained at steady state before and after lime injection.

For each attrition test, 0.5 kg of lime were initially injected so that the initial pressure drop in the reactor bed was about 15.24 cm of H_2O. During the test, the recirculating valve was closed to prevent the attritted fines captured by the first cyclone from entering the bed. At regular time intervals (30 min–20 h) the fluidization air was turned off, and the samples from the bed, the first cyclone, and second cyclone were immediately taken out. The collected samples were weighed, and thus the extent of attrition was obtained. The size distributions of bed material and attrited fines were also measured by a sieving method and a Coulter Counter (Model TA II, Coulter Electronics, Inc.), respectively. In addition, the samples were observed through a microscope and analyzed via an image analysis system.

Results and Discussion

Mechanical Attrition Tests. Attrition tests at room temperature were carried out with lime samples in a CFBA in a batch mode to see the fluid-induced attrition tendency. The fluidizing gas was air with superficial velocities from 2 to 5 m/s. Figure 3 shows the typical bed weight reductions of the parent solids with a MMD of 1764 μm due to attrition during fluidization in CFBA. The weight reduction occurs rapidly at the beginning of fluidization, continues, and finally levels off to reach a minimum weight, W_{min}, after 15 h. A similar trend was also noted by Shamlou et al. (1990) and Flamant and Chraibi (1989) for the attrition of agglomerates prepared from narrowly classified soda

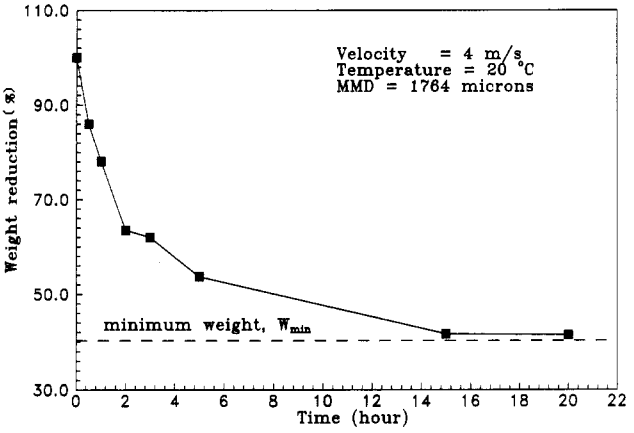

Figure 3. Typical attrition tendency of lime in a CFBA.

glass beads and manganese chloride particles, respectively. All other attrition tendencies obtained from attrition tests in CFBA closely follows the trends as shown in Figure 3. The results clearly imply a rounding off of the sharp edges and corners of the particles during initial fluidization, and a surface abrasion process at later fluidization.

The rounding off and surface abrasion of bed materials were also observed with a microscope as illustrated in Figure 4. Figure 4 shows the rough and irregular surface of the raw samples and the abraded surface of the parent solids after 10 min, 30 min, 1 h, and 5 h of fluidization with a superficial gas velocity of 2.5 m/s. The sharp edges gradually disappear, maintaining the same sphericity, and the surface becomes rougher and rougher with time due to collisions. The BET surface area of the parent solids as shown in Figure 5appears to increase slightly due to collisions as the fluidization continues and thus indicates that the surface of the parent solids becomes rougher while the appearance seems to be smoother. The size distribution of the attrited fines and sphericity of the parent solids are shown in Figures 6 and Figure 7. The size of fines abraded and captured by the cyclones and filter during fluidization ranged between the least MMD of 6.5 μm at the filter and the largest MMD of 11.3 μm at the second cyclone. The sphericity of the parent solids appeared to remain constant with time. The results as well as the visual observations clearly indicate that the predominant mechanism of lime attrition is surface abrasion resulting from collisions of the parent solids in the bed during fluidization.

The effect of the initial solid concentration in the bed on attrition is shown in Figure 8. The measurements were obtained with a gas velocity of 4 m/s for lime 1 and 2 m/s for lime 2. Evidently, attrition increases proportionally due to collisions of the parent solids until the initial solid concentration reaches a critical point. After the critical point, $C_{s,crit}$, attrition appears to be constant with regard to solid concentration in the bed. Therefore, the following conditions exist

at $C_s < C_{s,crit}$,

k_a is a function of the mass of bed materials

at $C_s \geq C_{s,crit}$,

k_a is independent of the mass of bed materials

where C_s is solid weight (kg/m^3) and k_a is the attrition rate constant (s^{-1}) but may be a function of the type of solids and fluidizing parameters.

The effect of gas velocity on attrition during fluidization is illustrated in Figure 9. Figure 9 shows that as the gas velocity increases, the extent of attrition significantly increases. The extent of attrition was defined as

$$x_a = \left(1 - \frac{W}{W_o}\right)100 \qquad (1)$$

where x_a is the extent of attrition of lime (%), W is the weight (kg) of parent solids in a bed measured at time t (s), and W_o is the initial weight (kg).

Thermal Attrition Tests. Since temperature affects the properties of solid sorbents such as the hardness and density as well as those of the fluidizing gas, some solids may be easily attrited at low temperature or others may soften or become brittle at high temperature. Flamant and Chraibi (1989) observed the slightly increasing attrition rate of manganese chloride particles with rising temperatures to 300 °C. Ulerich et al. (1980) also found that as temperature increases to 815 °C with the heating rate of 400 °C/min, the rate of limestone attrition increases. They suggested that the strength of limestone decreases at higher temperatures and leads to the higher rate of limestone attrition during calcination of the limestone. But lime is extremely hygroscopic and absorbs moisture from the air to become hydrated lime for which its hardness is less than that of lime. As the temperature increases, hydration may slow due to the evaporation of moisture, and thus lime may become less fragile. In addition to hydration, recarbonation of lime occurs rapidly at room temperature in the presence of moisture. The recarbonation can occur slowly in arid climates of 15% relative humidity even though the volume of CO_2 in the atmosphere is only about 0.03% (Boynton, 1980). Also, surface layers of hydrated lime may react at higher rates with ambient CO_2 concentrations at higher temperatures providing a more dense layer of carbonate which will tend to retard attrition. Carbonation hardens the lime, and this reaction rate accelerates with rising temperature. Therefore, thermal attrition of lime may be different from the common attrition trends observed by others for limestone.

The temperature effect on lime attrition during fluidization is represented in Figure 10. It clearly shows that the extent of lime attrition exponentially decreases as temperature increases up to 177 °C. The results suggest that thermal attrition of lime may strongly depend on the hardness changes due to carbonation and hydration rather than the decrepitations resulting from the increase of internal pressure with rising temperatures as observed commonly in such solids as limestones and coals.

Modeling of Attrition Rate Constants. The experimental data presented in Figure 3 suggest an exponential decrease of the weight of parent solids in a bed during fluidization. Other investigators (Lin et al., 1980; Shamlou et al., 1990; Jiang, 1991) have applied a first-order attrition model to estimate the weight changes of bed materials in a fluidized bed, but the extent of attrition obtained experimentally did not follow exactly the attrition model for operations longer than 1 h. On the basis of these findings, a first-order attrition model considering the minimum weight as shown in Figure 3 is suggested as follows

$$\frac{dw}{dt} = -k_a(W - W_{min}) \qquad (2)$$

where W is the weight of the parent solids in the bed (kg), W_{min} is the minimum weight below which attrition may be essentially negligible, and k_a is the attrition rate constant (s^{-1}). Integrating eq 2 with the boundary conditions of $t = 0$, $W = W_o$, and $t = t$, $W = W$, gives

(a) Raw lime sample

(b) Lime after 10 minutes attrtion

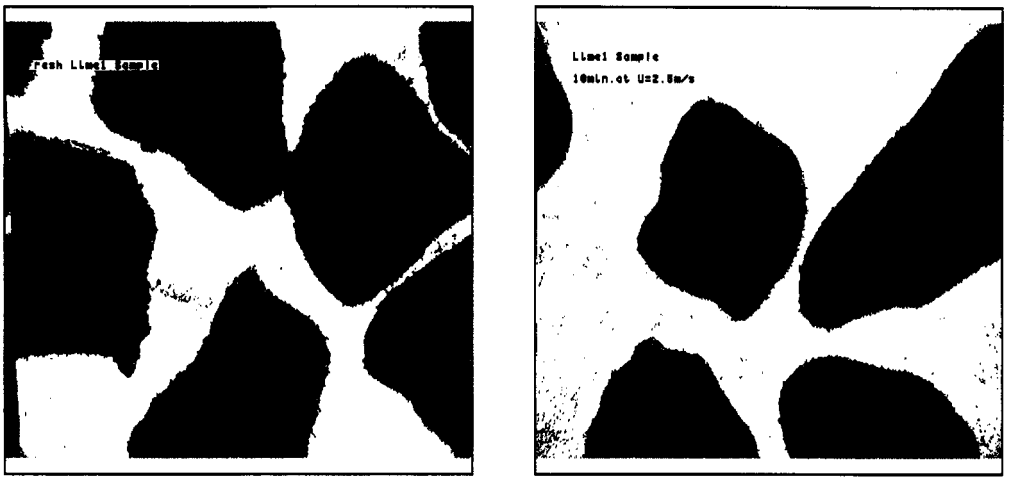

(c) Lime after 60 minutes attrition

(d) Lime after 300 minutes attrition

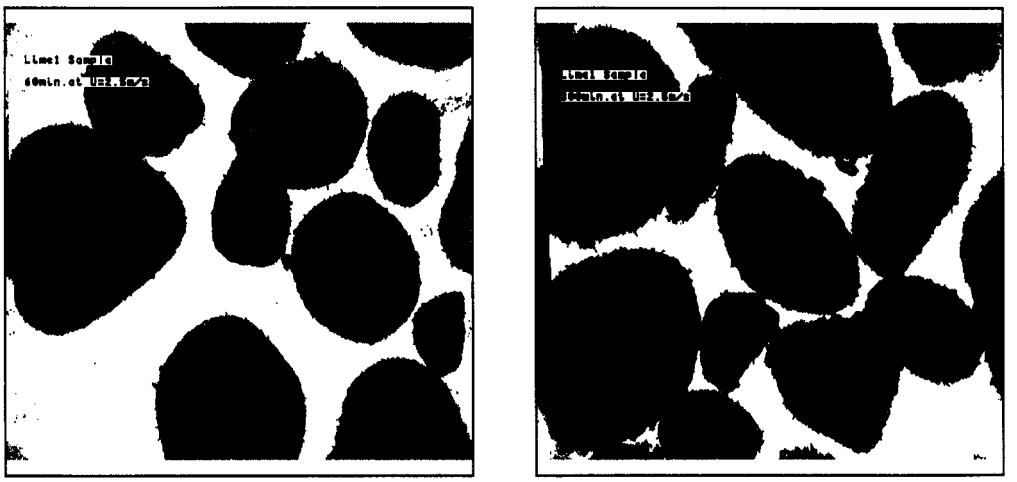

Figure 4. Microscopic observations of parent solids after fluidization in CFBA.

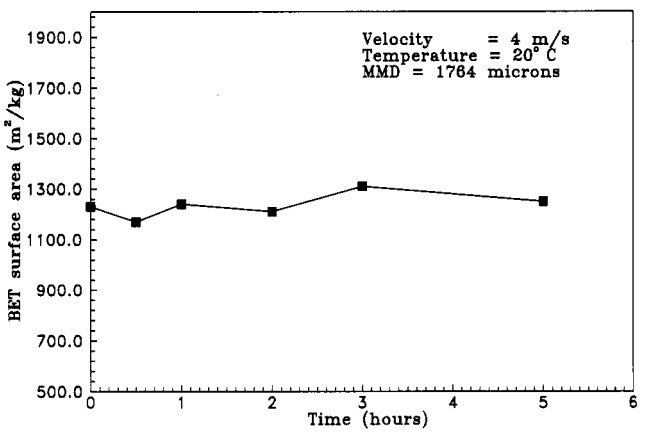

Figure 5. Effect of attrition on BET surface area of lime.

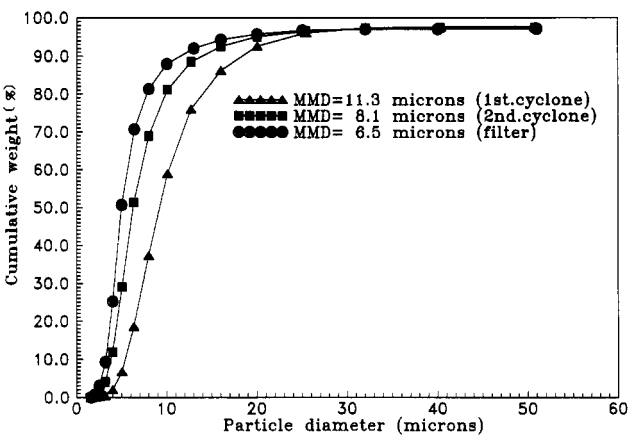

Figure 6. Size distribution of fines collected by cyclones and filter.

$$\ln\left(\frac{W - W_{min}}{W_o - W_{min}}\right) = -k_a t \qquad (3)$$

The attrition rate constant, k_a, therefore, can be obtained from the slope of plotting ln $[(W - W_{min})/(W_o - W_{min})]$ versus time, t. The results are shown in Figure 11 for fluidization time to 5 h. The attrition rate constants, k_a, obtained from the curves are 0.0018 s^{-1} for 2 m/s, 0.0038 s^{-1} for 3 m/s, 0.0055 s^{-1} for 4 m/s, and 0.0080 s^{-1} for 5 m/s.

The attrition rate constant, k_a, depends upon the fluid-dynamic induced forces acting on the particles. The attrition rate has been assumed to be directly proportional to the excess energy of the gas above the minimum fluidization velocity by many investigators (Merrik and Highly, 1974; Lin et al., 1980; Flamant and Chraibi, 1989) or related to the energy transformation from the fluid to the particle (Ray et al., 1987; Shamlou et al., 1990). For

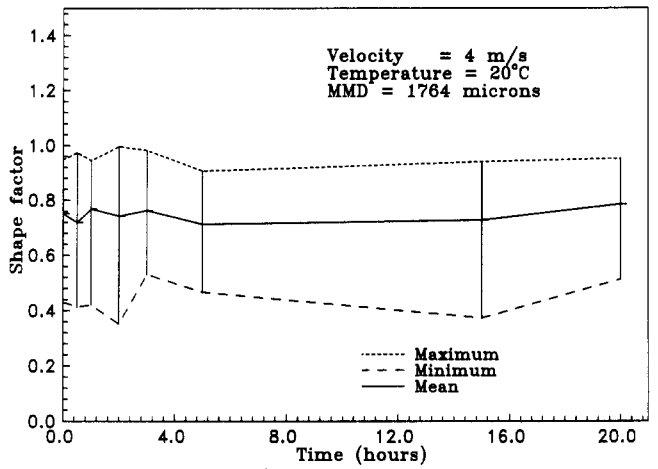

Figure 7. Measurements of shape factor of solids after attrition.

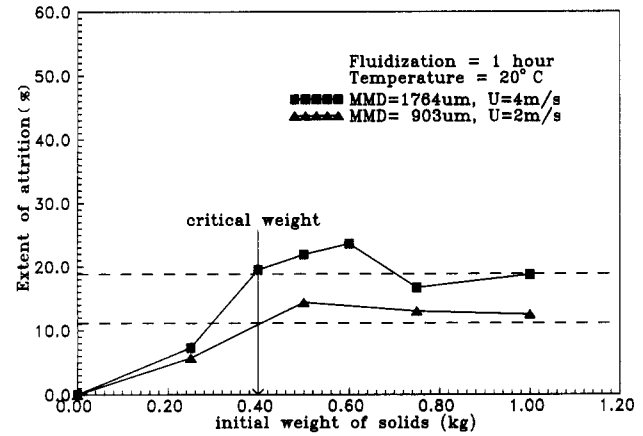

Figure 8. Effect of initial weights on lime attrition.

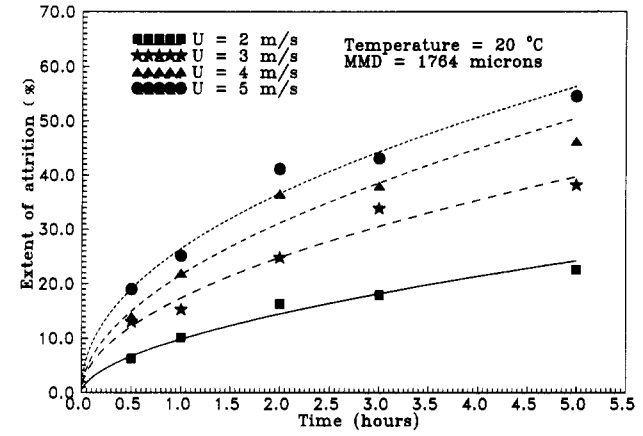

Figure 9. Effect of gas velocity on the extent of lime attrition.

fluid–dynamic induced attrition only, attrition may be proportional to the excess energy, E_{exc} which is defined as

$$E_{exc} = A(U - U_{mf})\Delta p = Wg(U - U_{mf}) \qquad (4)$$

where A is the cross sectional area of the reactor (m^2), U the superficial gas velocity (m/s), and U_{mf} the minimum fluidization velocity (m/s), W the weight of parent solids in a bed (kg), Δp the total pressure drop of the bed (kg/m·s^2), and g the gravitational constant (m/s^2). When the superficial gas velocity, U is equal to or becomes less than the minimum fluidization velocity, U_{mf}, attrition may be neglected. But such an assumption may not be reasonable for cases where the attrition process still occurs by chemical reaction or thermal attrition even when the gas velocity is equal to or less than the minimum fluidization velocity.

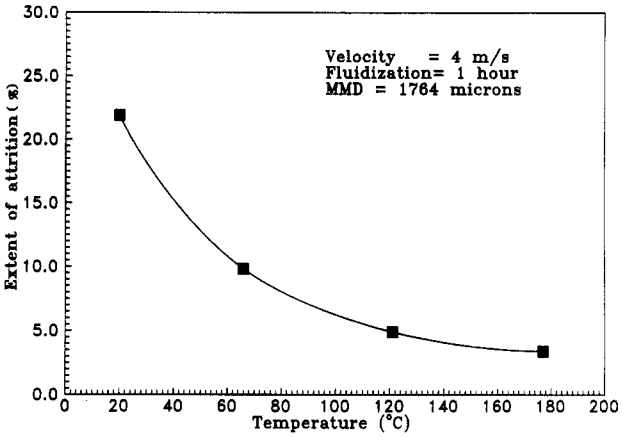

Figure 10. Effect of temperature on lime attrition.

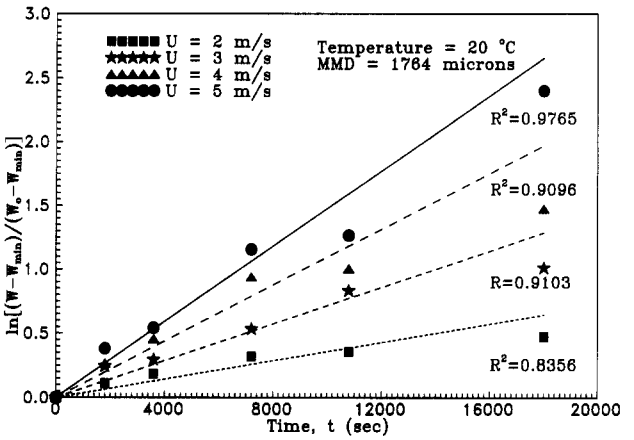

Figure 11. Attrition rate constants of lime at different velocities.

Since the rate of attrition increases rapidly with rising gas velocity as shown in Figure 9, and the relative effect of an increase of gas velocity diminishes as the temperature is raised, the relationship between the attrition rate constant and the gas velocity may be expressed as an Arrhenius form. Moreover, the gas velocity may be expressed in terms of the energy supplied by the fluidizing gas into a bed reactor. Thus, the attrition rate constant in an Arrhenius form is written as

$$k_a = k_0 \exp\left(-\frac{E_a}{\psi}\right) \qquad (5)$$

where E_a is the pseudoattrition activation energy (kJ/kg) and will be specific to the material undergoing attrition, ψ is the energy supplied by the fluidizing gas to the dense zone per unit mass of the solids in the dense zone (kJ/kg), and k_0 is the frequency factor (specific to the material undergoing attrition) which does not affect the sensitivity of attrition rates to gas velocities. The activation energy, E_a, represents the quantity of energy required to activate 1 kg of parent solids to a state sufficiently above the average energy level of the solids for which attrition may occur. The ratio of the energy supplied by the fluidizing gas to the mass of parent solids, ψ, is defined as

$$\psi = \frac{\text{energy supplied by the fluidizing gas}}{\text{mass of parent solids in a bed}}$$

The energy supplied to the dense zone, $\mathcal{P}$, is the total fluid energy above the condition of minimum fluidization and is given by

$$\text{energy supplied, } \mathcal{P} = M_g\left(\frac{U - U_{mf}}{\epsilon}\right)H \qquad (6)$$

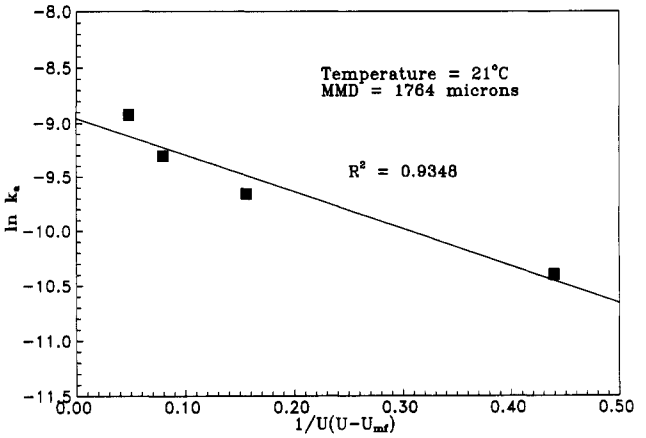

Figure 12. Arrhenius form for attrition rate constant.

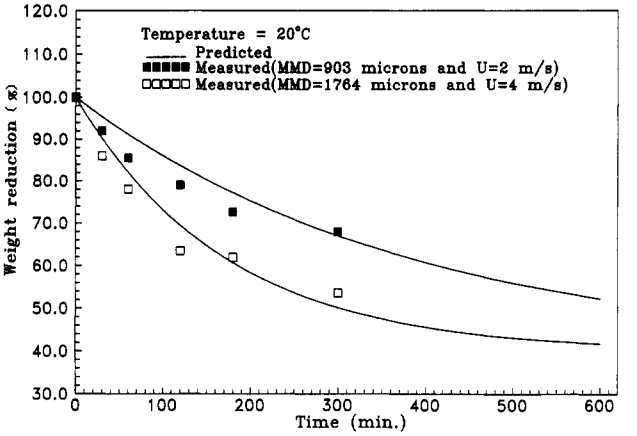

Figure 13. Comparison of weight changes calculated and measured.

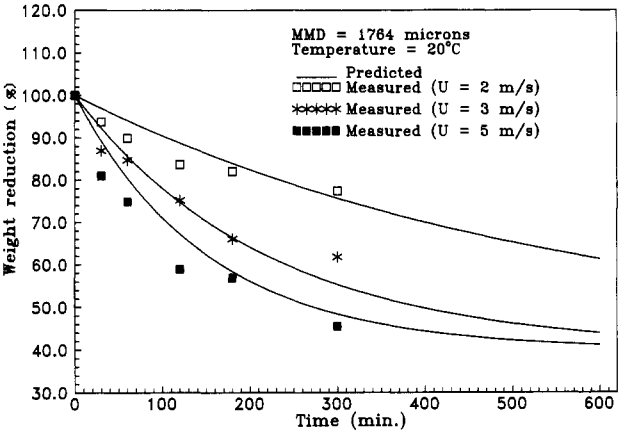

Figure 14. Comparison of weight changes calculated and measured.

where M_g is mass flow rate of gas (kg/s), U the superficial velocity of gas (m/s), ϵ the bed voidage, and H the height of the dense zone (m). Replacing the mass flow rate of gas with $M_g=(PQM_w)/(RT)$, and $Q = UA$, eq 6 may be written as

$$\mathcal{P} = \frac{PM_wAHU(U - U_{mf})}{RT\epsilon} \tag{7}$$

where P is the average absolute pressure (kg/m·s^2); M_w the molecular weight of gas (kg/kg-mol), A the cross-sectional area of bed (m^2), R the universal gas constant (kJ/kg-mol·K), and T the temperature (K). With substitution of eq 7 into eq 5, the following equation is obtained

$$k_a = k_o \exp\left[-\frac{E_aRT\epsilon M_s}{PM_wAHU(U - U_{mf})}\right] \tag{8}$$

where M_s is the mass of parent solids in a bed (kg). If we consider the critical point above which attrition becomes independent of bed mass, the mass of solids, M_s, may be replaced with $C_{s,crit}(AH_b)$. [The value of $C_{s,crit}$ represents the minimum bed weight where particle collisions represent the predominant attriting mechanism and is (in all likelihood) a complex function of the bed geometry and the type of attriting material.] The height of the dense zone, H, is also replaced with ϵH_b, where H_b is the height of bed reactor (m). Then, the above equation is written as

$$k_a = k_o \exp\left[-\frac{E_aRTC_{s,crit}}{PM_wU(U - U_{mf})}\right] \tag{9}$$

Equation 9 suggests that the attrition rate constant is affected by the gas properties such as temperature and molecular weight as well as the fluidization velocity. The size of parent solids also affects the attrition rate since the minimum fluidization velocity varies with size of bed solids. Finally, the weight reduction of the parent solids during fluidization in a bed may be obtained by differentiating eq 2 with the attrition rate constant, k_a:

$$W = (W_0 - W_{min})e^{-k_at} + W_{min} \tag{10}$$

Equations 9 and 10 with the experimental attrition data mentioned previously provide a means of evaluating the extent of attrition during long term fluidization over wide gas velocities, temperatures, and solid size ranges.

The experimental data obtained from the present attrition tests were compared with the attrition model considering thermal attrition, as described in eqs 9 and 10. The linear relationship between ln k_a and $-1/U(U - U_{mf})$ as shown in Figure 12 indicates that the attrition rate constant, k_a, may be expressed in an Arrhenius form, and from the slope the attrition activation energy, E_a and k_o, can be obtained as $E_a = 3.383 \times 10^{-3}$ kJ/kg and $k_o = 1.29 \times 10^{-4}$ s^{-1}. The comparisons of the mechanical attrition data obtained experimentally with the theoretical values computed with the attrition activation energy and k_o are illustrated in Figures 13 and 14. Two different sizes of lime (MMD = 903 and 1764 μm) are applied for verifying the attrition model, and the results are shown in Figure 13. Figure 14 represents the weight reduction due to attrition at three different velocities (2, 3, and 5 m/s). The theoretical weight loss of solids during fluidization at different gas velocities and solid sizes is in good agreement with observations. However, eqs 9 and 10 underestimate the weight reduction at different temperature as shown in Table III. The results suggest that the attrition rate may be affected by solid properties as well as gas properties as temperature increases. Lime is hygroscopic and absorbs moisture from the air, and its hardness increases with increasing temperature. As the temperature increases, dehydration and recarbonation occur and the particles become less fragile. Such property changes may significantly affect the attrition of solids at higher temperatures.

Table III. Attrition of Lime at Different Temperatures

	wt reductn (%) after 1 h of fluidization	
T (°C)	calcd by eq 10	measured exptlly
65	82.7	90
121	83.5	95
177	84.2	96.4

Conclusions

Attrition of lime sorbent plays a very important role for its utilization in dry lime injection FGD processes. The

experimental data of lime sorbent attrition obtained from mechanical and thermal attrition tests in a circulating fluidized bed absorber (CFBA) are represented. The results indicate that the predominant attrition mechanism during lime fluidization is the surface abrasion due to the collisions of the parent solids in a bed. The thermal attrition of lime decreased possibly due to its hardened properties with rising temperatures while such solids as limestone become more attrittable by crepitation resulting from increased internal pressure. With an introduction of the minimum weight of parent solids, the attrition rate of lime in a CFBA has a first-order dependency with respect to time. The attrition rate constant is expressed in an Arrhenius form, using the kinetic model which relates the attrition rate to the gas properties such as temperature and molecular weight and the geometry of the fluidized bed as well as the fluidization velocity. The experimental data obtained from the present attrition tests in a CFBA agree well with the attrition model considering thermal attrition. From the model the attrition activation energy, E_a and k_o, can be obtained as $E_a = 3.383 \times 10^{-3}$ kJ/kg and $k_o = 1.29 \times 10^{-4}$ s^{-1}. The comparisons of the mechanical and thermal attrition data obtained experimentally with the theoretical values computed with the attrition activation energy and k_o are in good agreement. The attrition activation energy and rate constants were obtained with a commercialized lime and are specific to lime and not to other materials. It may not be applied to fluidization of other materials but may be applicable to lime fluidization.

Acknowledgment

The authors would like to express their appreciation to Dravo Lime Co. for supplying the sorbent material used in this study. Support from the Ohio Coal Development Office through Grant OCRC/91-1.7 and the U.S. Department of Energy through Grant FG-22-91PC91336 for this research are gratefully acknowledged.

Nomenclature

A = cross-sectional area of bed reactor, m^2
C_s = weight of solids in a bed, kg/m^3
$C_{s,crit}$ = critical weight of solids in Figure 5
E_a = attrition activation energy, kJ/kg
E_{exc} = excess energy by the gas velocity above minimum fluidization velocity, m/s
g = gravitational constant, cm/s^2
H = height of dense zone in a bed, m
H_b = height of bed reactor, m
H_{mf} = height of dense zone at minimum fluidization velocity, m
k_a = attrition rate constant, s^{-1}
k_w = attrition rate constant under wet conditions, s^{-1}
k_o = frequency factor in an Arrhenius form
M_g = mass flow rate of fluidizing gas, kg/s
M_s = mass of solids, kg
M_w = molecular weight of gas, kg/kg-mol
P = absolute pressure of gas, kg/m·s^2
ΔP = pressure drop of bed reactor, kg/m·s^2
Q = volumetric flow rate of gas, m^3/s
R = gas constant, kJ/kg-molK
t = time, s
Δt = approach to saturation temperature, °C
T = temperature, K
U = superficial gas velocity, m/s
U_{mf} = minimum fluidization velocity, m/s
W = weight of solids, kg
W_o = initial weight of solids, kg
W_{min} = minimum weight of parent solids in a bed, kg
X_a = extent of attrition, %

Greek Letters

ψ = ratio of the energy supplied by the gas to the mass of solids in eq 6
$\mathcal{P}$ = energy supplied by fluidizing gas, kJ
ϵ = bed voidage

Literature Cited

Arena, U. M.; D'Amore, M.; Massimilla, L. Carbon Attrition During the Fluidized Combustion of a Coal. *AIChE J.* **1983**, *29*, 40–49.

Bemrose, C. R.; Bridgwater, J. A Review of Attrition Test Methods. *Powder Technol.* **1987**, *2*, 97–126.

Borgwardt, R. H.; Bruce, K. R. Effect of Specific Surface Area on the Reactivity of CaO with SO_2. *AIChE J.* **1986**, *32*, 239–246.

Boynton, R. S. Definitions and Properties of Limes. *Chemistry and Technology of Lime and Limestone*, 2nd ed.; John Wiley & Sons; New York, 1980; pp 193–227.

British Material Handling Board. Attrition Dynamics. *Particle Attrition: State-of-the-art review*, Series on Bulk Materials Handling; Trans Tech Publications: Aedermannsdorf, 1987; pp 3–19.

Chirone, R.; D'Amore, M.; Massimilla, L. Carbon Attrition in the Fluidized Combustion of a Petroleum Coke. Twentieth Symposium (International) on Combustion; *The Combustion Institute*: Pittsburgh, PA, 1984; pp 1505–1511.

Flamant, G.; Chraibi, M. A. Kinetic, Thermal and Chemical Attrition of Manganese Chloride Particles in a Fluidized Bed. *Powder Technol.* **1989**, *59*, 97–107.

Jiang, X. The Role of Humidification and Attrition on Sulfur Dioxide Removal in a Circulating Fluidized Bed Absorber. Ph.D. Dissertation, The University of Cincinnati, 1991.

Keener, T. C.; Jiang, X. L.; Hao, J. Test Results on the Use of A Circulating Fluidized Bed Absorber (CFBA) for Control of SO_2. EPA/EPRI Cosponsored First Combined FGD and Dry SO_2 Control Symposium: St. Louis, MO October 1988.

Keener, T. C.; Lee, S. K.; Khang, S. J. The Effect of Attrition on Sorbent Utilization. Final Report OCRC/91-1.7; The Ohio Coal Development Office: Columbus, OH, 1991.

Kirchgessner, D. A.; Hendriks, R. V.; Kaplan, N. Calcium-Based Sorbents in the LIMB Process. EPA/600/D-87/136; U.S. EPA, Air and Energy Engineering Research Laboratory, Research Triangle Park, NC; April 1987.

Lin, L.; Sears, J. T.; Wen, C. Y. Elutriation and Attrition of Char from a Large Fluidized Bed. *Powder Technol.* **1980**, *27*, 105–115.

Merrick, D.; Highley, J. Particle Size Reduction and Elutriation In a Fluidized Bed Process. *AIChE Symp. Ser.* **1974**, *70*, 361–378.

Ray, Y. C.; Jiang, T. S.; Wen, C. Y. Particle Attrition Phenomena in a Fluidized Bed. *Powder Technol.* **1987**, *49*, 193–206.

Ray, Y. C.; Jiang, T. S.; Jiang, T. L. Particle Population Model for a Fluidized Bed with Attrition. *Powder Technol.* **1987**, *52*, 35–48.

Shamlou, P. A.; Liu, Z.; Yates, J. G. Hydrodynamic Influences on Particle Breakage in Fluidized Bed. *Chem. Eng. Sci.* **1990**, *45*, 809–817.

Ulerich, N. H.; Vaux, W. G.; Newby, R. A.; Keairns, D. L. Experimental/Engineering Support for EPA;s PBC Program. Final Report EPA-600/7-80-015A; Westinghouse Research & Development Center; Pittsburgh, Jan 1980.

Vaux, W. G.; Fellers, A. W. Measurement of Attrition Tendency in Fluidization. *AIChE Symp. Ser.* **1981**, *205*, 107–115.

Received for review January 5, 1993
Revised manuscript received May 11, 1993
Accepted July 7, 1993[⊗]

[⊗] Abstract published in *Advance ACS Abstracts*, October 1, 1993.